A novel immunofluorescence method to visualize microtubules in the antiparallel overlaps of microtubule-plus ends in the anaphase and telophase midzone

Aya Ifuji, Takahisa Kuga, Yuichiro Kaibori, Youhei Saito, Yuji Nakayama*

Department of Biochemistry & Molecular Biology, Kyoto Pharmaceutical University, Kyoto 607-8414, Japan

ABSTRACT

Cell division, in which duplicated chromosomes are separated into two daughter cells, is the most dynamic event during cell proliferation. Chromosome movement is powered mainly by microtubules, which vary in morphology and are organized into characteristic structures according to mitotic progression. During the later stages of mitosis, antiparallel microtubules form the spindle midzone, and the irregular formation of the midzone often leads to failure of cytokinesis, giving rise to the unequal segregation of chromosomes. However, it is difficult to analyze the morphology of these microtubules because microtubules in the antiparallel overlaps of microtubule-plus ends in the midzone are embedded in highly electron-dense matrices, impeding the access of anti-tubulin antibodies to their epitopes during immunofluorescence staining. Here, we developed a novel method to visualize selectively antiparallel microtubule overlaps in the midzone. When cells are air-dried before fixation, aligned α-tubulin staining is observed and colocalized with PRC1 in the center of the midzone of anaphase and telophase cells, suggesting that antiparallel microtubule overlaps can be visualized by this method. In air-dried cells, mCherry-α-tubulin fluorescence and β-tubulin staining show almost the same pattern as α-tubulin staining in the midzone, suggesting that the selective visualization of antiparallel microtubule overlaps in air-dried cells is not attributed to an alteration of the antigenicity of α-tubulin. Taxol treatment extends the microtubule filaments of the midzone in air-dried cells, and nocodazole treatment conversely decreases the number of microtubules, suggesting that unstable microtubules are depolymerized during the air-drying method. It is of note that the air-drying method enables the detection of the disruption of the midzone and premature midzone formation upon Aurora B and Plk1 inhibition, respectively. These results suggest that the air-drying method is suitable for visualizing microtubules in the antiparallel overlaps of microtubule-plus ends of the midzone and for detecting their effects on midzone formation.

1. Introduction

Microtubules are a major cytoskeleton filament in the cell and play essential roles in various intracellular processes, including the transport of membrane vesicles in the cytoplasm, cell motility, and chromosome movement during cell division [1–3]. Microtubules are polymers of a heterodimer of α- and β-tubulin, and have polarity; the end where β-tubulin is exposed is referred to as the plus end, and the opposite end, where α-tubulin is exposed, is referred to as the minus end [4]. The polymerization rate is higher at the plus end than at the minus end [5]. However, polymerization and depolymerization dynamics can be modified by microtubule-associated proteins to accomplish the biological functions of microtubules, and the regulation of these dynamics is pivotal to microtubule function [6–10].

Cell division, in which duplicated DNA is separated into two daughter cells, is the most dynamic event during cell proliferation. The mitotic spindle is the apparatus by which chromosomes are segregated and is composed of chromosomes and microtubules, by which chromosome movement is mainly powered. Microtubules vary in their morphology and are organized into characteristic structures according to mitotic progression. From the entry into mitosis to just before the onset of anaphase, microtubules are organized into three different types: kinetochore, astral, and interpolar microtubules. During anaphase and telophase, the spindle midzone, which consists of antiparallel microtubule bundles, forms and plays crucial roles in positioning and signaling for the assembly of the contractile ring. At the last step of cell

division, cytokinesis, the midbody forms and regulates the timing of abscission. A variety of microtubule-bound proteins organize microtubule structures by regulating the polymerization, depolymerization, and bundling of microtubules [11]. PRC1 [12], centralspindlin [13–15], CLASP [16–18], MKLP2 [19,20], and KIF4 [21–24] are core organizers of the spindle midzone and midbody, and are regulated by upstream kinases [25,26].

During mitosis, different populations of microtubules have distinct polymerization and depolymerization dynamics and stabilities. When centrosomes are positioned closely at the beginning of cell division, the kinesin Eg5 tethers the antiparallel microtubules and a pushing force generated by the slide of polymerizing antiparallel microtubules separates centrosomes [27–29]. Together with chromosome condensation and breakdown of the nuclear envelope, microtubules nucleated from centrosomes radiate microtubule-plus ends to capture chromosomes. By repeatedly extending and shrinking, namely, switching between polymerization and depolymerization, respectively, microtubules search for chromosomes. Once microtubules capture chromosomes, microtubules are stabilized [30]. Compared to astral microtubules, kinetochore microtubules are relatively stable against stimuli promoting depolymerization, such as low concentrations of nocodazole, a microtubule-depolymerizing agent [31], and low temperatures [32–34]. In anaphase B, the slide of elongating antiparallel microtubules of the midzone in opposite directions makes centrosomes move apart, resulting in spindle elongation [35–37]. At the final phase of cell division, microtubules of the central spindle and midbody are stabilized by their rigid bundling [12].

The microtubules in the spindle midzone play prerequisite roles in cytokinesis, and the midbody regulates abscission timing. Irregular formation of the spindle midzone and midbody during late mitosis often leads to a failure in cytokinesis, giving rise to the unequal segregation of chromosomes through the following cell cycle [38–42]. Thus, close analysis of these characteristic structures will give important insights into the regulation of cell division, especially cytokinesis and abscission. However, the microtubules in the antiparallel overlaps of microtubule-plus ends (sometimes referred to as "stem bodies") and Flemming body in the midbody are embedded in highly electron-dense matrices [43,44], impeding anti-tubulin antibodies from accessing their epitopes on microtubules during immunofluorescence staining and making it difficult to analyze the morphology of the overlapping antiparallel microtubules [44]. In the present study, we developed a novel immunofluorescence method to visualize selectively microtubules in the antiparallel overlaps of microtubule-plus ends in order to analyze the regulation of the spindle midzone.

2. Materials and methods

2.1. Cells

Human cervix adenocarcinoma HeLa S3 cells (Japanese Collection of Research Bioresources, Osaka, Japan) and pig kidney epithelial LLC-PK1 cells expressing both mCherry-tubulin and GFP-MKLP1 (provided by K. Kamijo) [45,46] were cultured in Dulbecco's modified Eagle's medium containing 5% fetal bovine serum with 20 mM HEPES-NaOH (pH 7.4) under an atmosphere of 5% CO_2 at 37 °C.

2.2. Chemicals

To modulate microtubule dynamics, Taxol (Wako, Kyoto, Japan), a microtubule-stabilizing agent, and nocodazole (Wako, Osaka, Japan), a microtubule depolymerizing agent, were used at 30 ng/mL for 10 min and 0.1 μg/mL for 10 min, respectively. To inhibit mitotic kinases, the Aurora B inhibitor ZM447439 (JS Research Chemical Trading, Wedel, Germany), the Plk1 inhibitor BI2536 (AdooQ BioScience, Irvine, CA, USA), and the Cdk1 inhibitor RO-3306 (Calbiochem, San Diego, CA,

USA) were used at 10 μM for 10 min, 0.1 μM for 10 min, and 8 μM for 20 h, respectively.

2.3. Antibodies

The following antibodies were used for immunofluorescence analysis: rat monoclonal anti-α-tubulin (1:1000–1:2000; MCA78G, Bio-Rad Laboratories, Hercules, CA, USA), rabbit monoclonal anti-β-tubulin (1:200; 9F3, Cell Signaling Technology, Danvers, MA, USA), rabbit polyclonal anti-PRC1 (1:300–1:500; H-70, Santa Cruz Biotechnology, Dallas, TX, USA), anti-γ-tubulin (1:200; Poly6209, BioLegend, San Diego, CA, USA), CREST, a human anti-centromere (1:400; HCT-0100, Immunovision, Springdale, AR, USA), and mouse monoclonal anti-AIM-1 (Aurora B) (1:300; 6/AIM-1, BD Biosciences, San Jose, CA, USA) antibodies. Alexa Fluor 488-, Alexa Fluor 555-, or Alexa Fluor 647-labeled donkey anti-mouse IgG, donkey anti-rabbit IgG, donkey anti-rat IgG, and FITC-anti-human secondary antibodies were used.

2.4. Immunofluorescence microscopy

The cells were fixed in phosphate-buffered saline (PBS) containing 4% formaldehyde for 20 min at room temperature, as described previously [47–49]. Alternatively, the culture medium was completely removed from the culture dish, and the cells were air-dried for 5 min, followed by fixation with PTEMF buffer (2 mM PIPES [pH 6.8], 0.2% Triton X-100, 10 mM EGTA, 1 mM $MgCl_2$, 4% formaldehyde) for 20 min at 30 °C. After fixation, the cells were permeabilized and blocked with PBS containing 0.1% saponin and 3% bovine serum albumin, and then incubated with primary and secondary antibodies. DNA was stained with 1 μM Hoechst 33342 for 1 h together with a secondary antibody. Fluorescence images were observed under an IX-83 fluorescence microscope (Olympus, Tokyo, Japan) equipped with a 60 × 1.42 NA oil-immersion objective (Olympus). The optical system for fluorescence observations included a U-FUNA cube (360–370 nm excitation, 420–460 nm emission) for observing Hoechst 33342 fluorescence, U-FBNA cube (470–495 nm excitation, 510–550 nm emission) for Alexa Fluor 488 fluorescence, U-FRFP cube (535–555 nm excitation, 570–625 nm emission) for Alexa Fluor 555 and mCherry fluorescence, and U-DM3-CY5 cube (600–650 nm excitation, 670–740 nm emission) for Alexa Fluor 647 fluorescence.

Confocal images were obtained using an LSM800 laser scanning microscope equipped with a 63 × 1.40 NA oil-immersion objective (Carl Zeiss, Jena, Germany). Hoechst 33342, Alexa Fluor 488, and Alexa Fluor 555 were excited with the 405-, 488-, and 561-nm line, and detected with 400–465 nm, 510–550 nm, and 570–620 nm emission filters, respectively.

Signal intensities of microtubule staining vary significantly according to mitotic sub-phase; therefore, imaging conditions were kept constant in each mitotic sub-phase but set independently of other sub-phases to avoid fluorescence overexposure. In addition, images in air-dried cells were contrast-enhanced (CE) to allow comparison of microtubles' morphology. Composite microscopic images were edited using ImageJ software (National Institutes of Health, Bethesda, MD, USA), GIMP software (https://www.gimp.org), and Illustrator CC software (Adobe, San Jose, CA, USA).

2.5. Cell synchronization

To synchronize the cells at the M phase, they were pre-arrested at the G2/M border by treatment with 8 μM RO-3306 for 20 h, washed with pre-warmed PBS (37 °C) supplemented with Ca^{2+} and Mg^{2+} (PBS [+]), and incubated in pre-warmed medium for 60 min, as described previously [49–51].

3. Results

3.1. Antiparallel microtubule overlaps in the spindle midzone are difficult to detect using a conventional immunostaining method

To investigate regulation of the spindle midzone, we thought that a method that could selectively visualize antiparallel microtubule overlaps in the spindle midzone would be advantageous. The spindle midzone is stabilized by the rigid bundling of antiparallel microtubules by the antiparallel microtubule-bundling protein PRC1 [12]. We first examined whether antiparallel microtubule overlaps could be visualized selectively by a conventional immunostaining method using anti-α-tubulin and anti-PRC1 antibodies. HeLa S3 cells were fixed with 4% formaldehyde (PTEMF buffer) and stained for α-tubulin and PRC1. PRC1 staining showed the highly ordered localization of PRC1 to a tight midline in the center of the midzone, indicating that antiparallel microtubule overlaps could be visualized by PRC1 staining (Fig. 1A). Yet, upon treatment with the Aurora B inhibitor ZM447439, PRC1 was localized diffusely along microtubules between the separating chromosomes. This is in agreement with a previous report that Aurora B promotes the interaction of PRC1 with KIF4A [52], and upon Aurora B inhibition, KIF4A fails to target to the midzone [52]. In the absence of KIF4, PRC1 is broadly diffused on the midzone [22]. Furthermore, during cytokinesis of cells with a monopolar spindle caused by the sequential addition of the Eg5 inhibitor STLC and then the Cdk1 inhibitor

RO-3306, PRC1 is localized at the monopolar midzone plus end; however, PRC1 is broadly diffused in the absence of KIF4 [22]. These results suggest that PRC1 is not restricted to the antiparallel microtubule overlaps in the spindle midzone in Aurora B-inhibited cells, and that PRC1 staining is not suitable for visualizing these microtubules when midzone-regulating proteins, including Aurora B and KIF4, are inhibited or malfunctioning.

While cold temperature has been shown to disrupt the mitotic spindle, certain microtubules of the mitotic apparatus are more resistant to cold treatment [32,53,54]: interpolar microtubules are disrupted by cold temperature; however, kinetochore microtubules and the midbody are more resistant [32]. In order to visualize antiparallel microtubule overlaps in the midzone, we examined whether midzone microtubules were resistant to cold treatment and could be detected by a conventional immunostaining method. Upon incubation of the cells on ice for 10 min, the interphase microtubule network almost completely disappeared (Fig. 1B). Metaphase kinetochore microtubules and anaphase half-spindles were observed, in agreement with a previous report [32], suggesting resistance to cold treatment. In sharp contrast, no microtubules were observed in the center of the midzone of anaphase and telophase cells. Although PRC1 staining was observed clearly in the absence of cold treatment, it was abolished by cold treatment. These results suggest that cold treatment is not suitable for visualization of the spindle midzone during anaphase and telophase.

Another way to depolymerize microtubules is by treating of cells
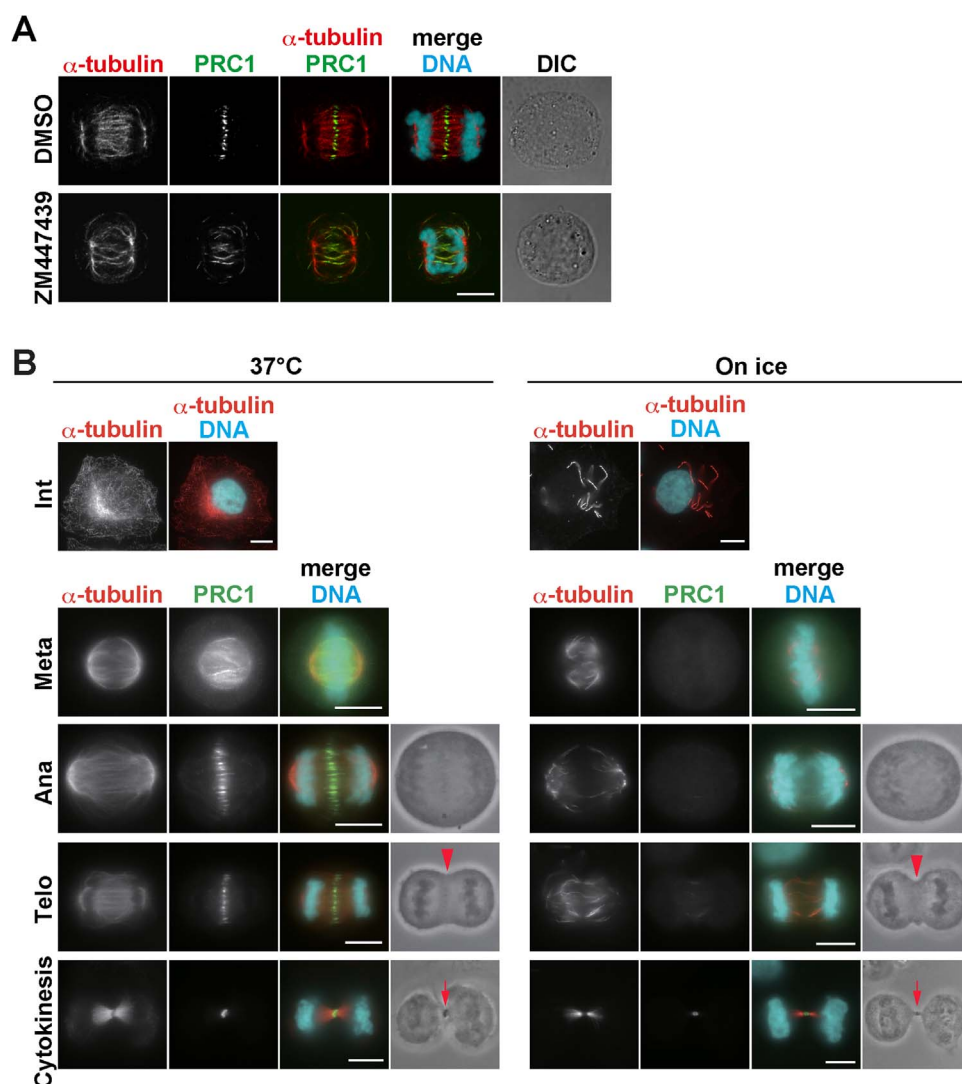
Fig. 1. Detection of microtubules after treatment with low temperature or low-concentration nocodazole. (**A**) HeLa S3 cells were treated with 8 μM RO-3306 for 20 h, washed free of RO-3306, and cultured in drug-free medium for 45 min. Subsequently, the cells were treated with DMSO (control) or 10 μM ZM447439 for 15 min. After fixation with PTEMF, the cells were stained for α-tubulin (red), PRC1 (green), and DNA (cyan). Confocal images show representative cells at anaphase. DIC, differential interference contrast. (**B**, **C**) HeLa S3 cells were incubated on ice or at 37 °C (control) for 10 min (**B**), or treated with 30 ng/mL nocodazole or DMSO (control) at 37 °C for 10 min (**C**). After fixation with PBS(-), they were stained for α-tubulin (red), PRC1 (green), and DNA (cyan). Images show representative cells at interphase (Int), metaphase (Meta), anaphase (Ana), telophase (Telo), and cytokinesis. Anaphase and telophase were distinguished according to the absence (anaphase) or presence (telophase) of ingression of the cleavage furrow (arrowheads). Cells with a midbody (arrows) were classified into the cytokinesis phase. Scale bars, 10 μm. (**D**) HeLa S3 cells were treated with 8 μM RO-3306 for 20 h, washed free of RO-3306, and cultured in drug-free medium for 50 min. Subsequently, the cells were treated with 30 ng/mL nocodazole or DMSO (control) at 37 °C for 10 min and fixed with PBS(-), followed by staining for α-tubulin (red) and DNA (cyan). The mitotic cells were classified into three groups: before anaphase onset (Pro/Prometa/Meta), in both anaphase and telophase (Ana/Telo), or in cytokinesis. The percentages within mitotic cells are plotted as mean ± S.D. from more than four independent experiments. In each experiment, at least 128 cells were examined. P-values were calculated by Student's *t*-test. N.S., not significant.
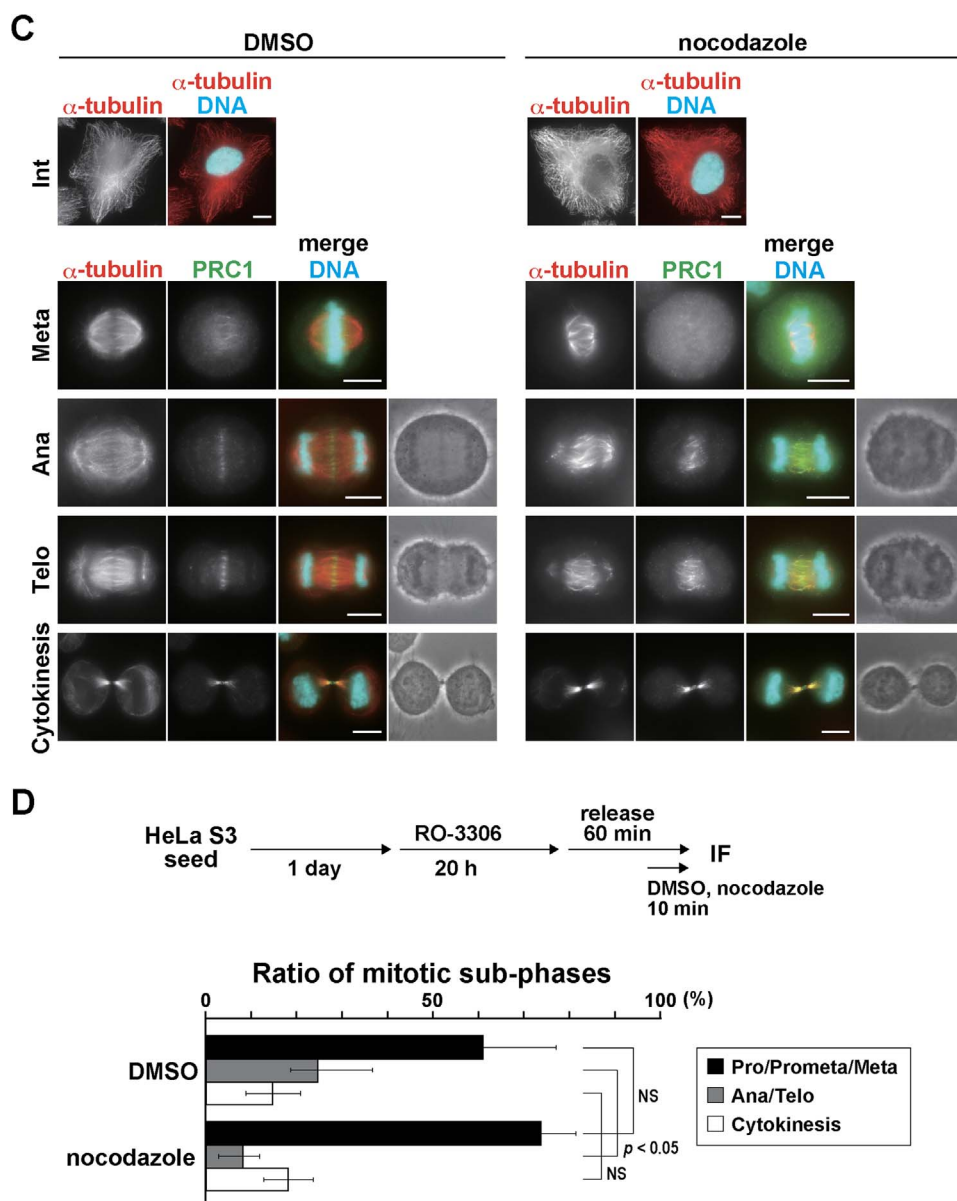
C

D

with the microtubule-depolymerizing agent nocodazole. The sensitivities to nocodazole are different in subpopulations of microtubules [31]. We, thus, treated the cells with a low concentration of nocodazole (30 ng/mL) for 10 min and stained for α-tubulin in mitotic cells. The nocodazole concentration used here is lower than that generally used for cell cycle arrest. Even when the cells were treated with nocodazole, no noticeable changes were observed in α-tubulin staining of interphase cells (Fig. 1C). In nocodazole-treated mitotic cells, the bipolar spindle during metaphase, microtubules of the midzone during anaphase and telophase, and midbody microtubules, but not astral microtubules, were observed. PRC1 staining was also observed in cells after the onset of anaphase; however, PRC1 was diffusely localized along microtubules between the separating chromosomes, as observed in cells treated with ZM447439, an Aurora B inhibitor. To examine the effect of a low concentration of nocodazole on mitotic progression, the cells were arrested at the G2/M border with the Cdk1 inhibitor RO-3306 and mitotic progression was estimated after washing the cells free of RO-3306 and a following 60-min incubation in medium in the presence or absence of nocodazole. Microscopic analysis of cells stained for α-tubulin and DNA showed that the number of anaphase and telophase cells was significantly decreased (Fig. 1D). These results suggest that nocodazole

treatment, in addition to cold treatment, is not suitable for the visualization of antiparallel microtubule overlaps, prompting us to develop a new method to visualize them selectively without affecting mitotic progression.

3.2. Air-drying before fixation enables the visualization of antiparallel microtubule overlaps

In order to visualize antiparallel microtubule overlaps, we fixed the cells using three different methods: 4% formaldehyde, 100% methanol, and 10% trichloroacetic acid (TCA). However, α-tubulin staining showed that these methods were not suitable for staining antiparallel microtubule overlaps. Intriguingly, when the cells were air-dried for 5 min before fixation, aligned α-tubulin staining was observed in the center of the anaphase and telophase midzone (Fig. 2A, air-dried, Supplemental Fig. S1), suggesting that antiparallel microtubule overlaps can be visualized in air-dried cells in spite of the lower fluorescence intensities. Additionally, kinetochore microtubules and the Flemming body in the midbody were also observed in the air-dried cells. It is noteworthy that longer exposure of the cells to air, such as for 20 min, weakened the fluorescence intensity of antiparallel microtubule
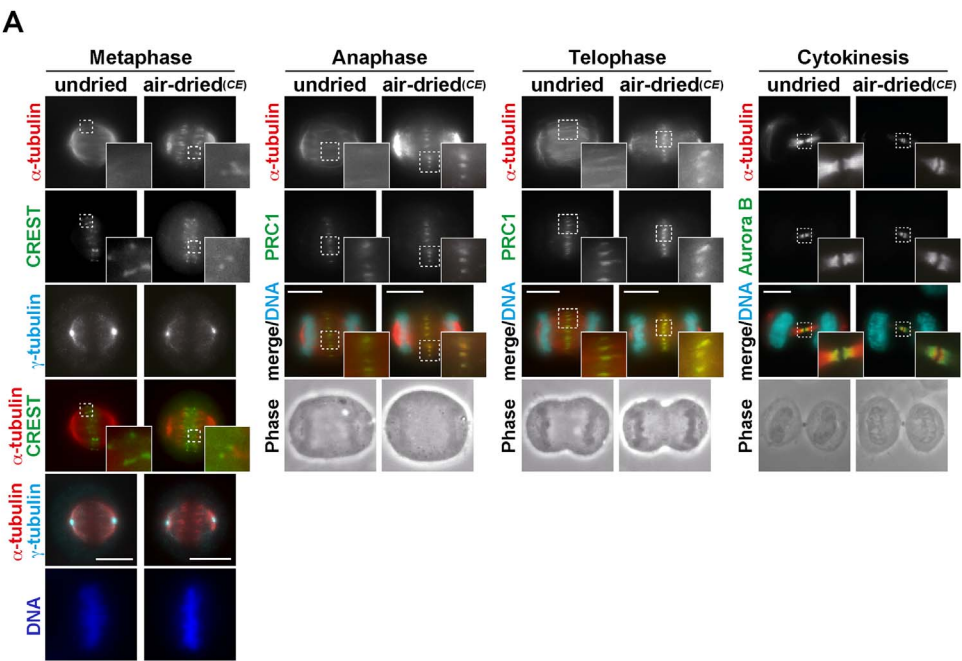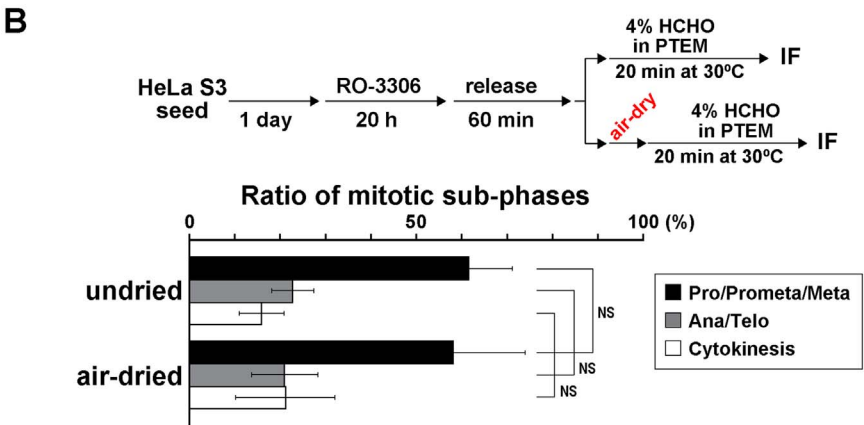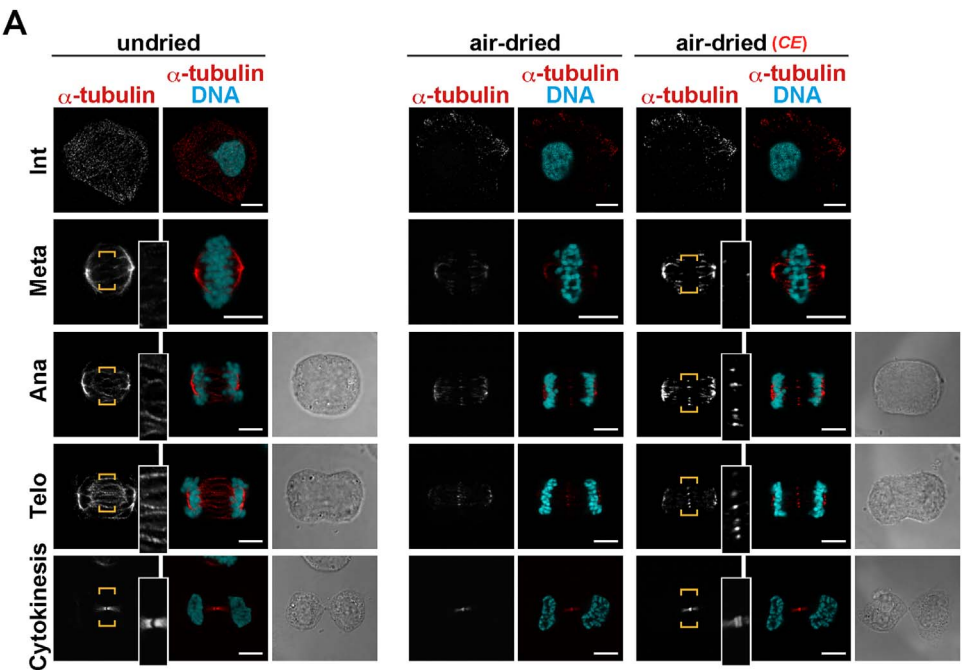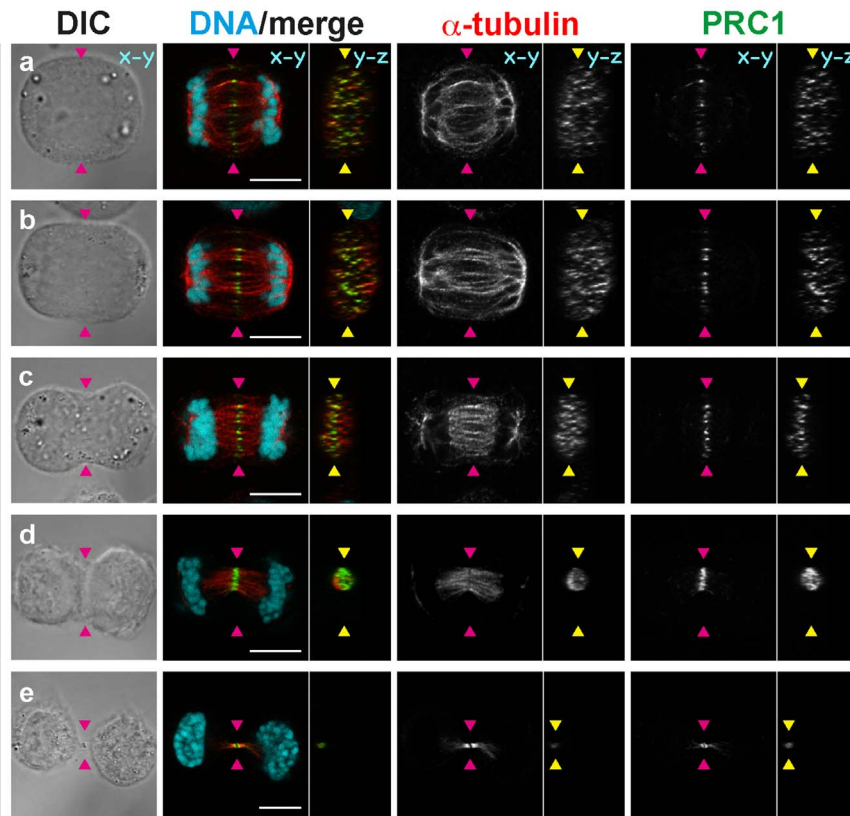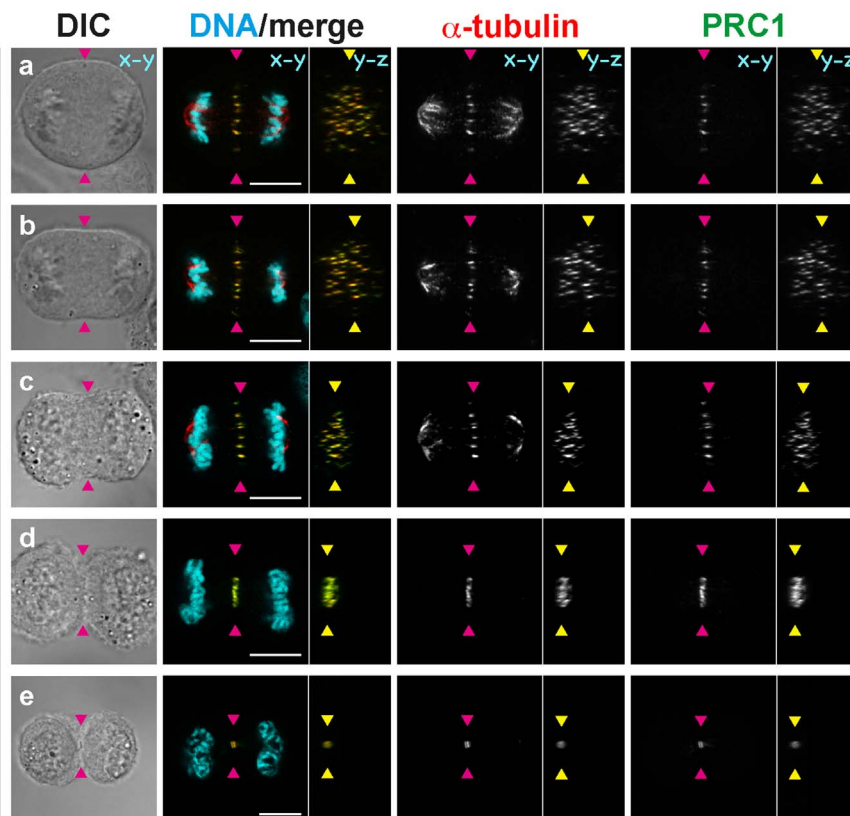
Fig. 2. Detection of midzone microtubules in air-dried cells without affecting mitotic progression. (**A**) HeLa S3 cells were air-dried for 5 min or undried, fixed with PTEMF, and stained for α-tubulin (red) and DNA (cyan). Confocal images show representative cells at interphase or the indicated sub-phases of mitosis. While the images were obtained under a constant setting for the same mitotic sub-phase, the microtubule fluorescence of air-dried cells was contrast-enhanced (**CE**) to allow comparison of the intensity and morphology of α-tubulin staining between air-dried and undried cells. Magnified images at the center of mitotic cells are shown. The cells were classified into mitotic sub-phases as described in Fig. 1. DIC, differential interference contrast. Scale bars, 10 μm. (**B**) HeLa S3 cells were treated with 8 μM RO-3306 for 20 h, washed free of RO-3306, and cultured in drug-free medium for 60 min. The cells were air-dried or undried, fixed, and stained for α-tubulin (red) and DNA (cyan). The mitotic cells were classified into three groups: before anaphase onset (Pro/Prometa/Meta), in both anaphase and telophase (Ana/Telo), or in cytokinesis. The percentages within mitotic cells are plotted as mean ± S.D. from more than four independent experiments. In each experiment, at least 179 cells were examined. P-values were calculated by Student's t-test. N.S., not significant.

Fig. 3. Air-drying before fixation enables the detection of antiparallel microtubule overlaps. (**A**) HeLa S3 cells were air-dried for 5 min or undried and fixed with PTEMF. Metaphase cells stained for α-tubulin (red), kinetochore (CREST, green), γ-tubulin (cyan), and DNA (blue) are shown. Anaphase and telophase cells stained for α-tubulin (red), PRC1 (green), and DNA (cyan) are shown. Cytokinesis cells stained for α-tubulin (red), Aurora B (green), and DNA (cyan) are shown. The microtubule fluorescence of air-dried cells was contrast-enhanced (**CE**). Magnified images of the dotted area are shown. In anaphase, telophase, and cytokinesis, phase-contrast images of cells are shown (right). The cells were classified into mitotic sub-phases as described in Fig. 1. Scale bars, 10 μm. (**B**) HeLa S3 cells were air-dried for 5 min or undried and fixed with PTEMF. Anaphase, telophase, and cytokinesis cells stained for α-tubulin (red), PRC1 (green), and DNA (cyan) were analyzed by confocal microscopy. z-stack images were acquired at 0.3-μm intervals, and images of the middle focal planes (x-y) and lateral cross-sectional views (y-z) constructed from the z-stack images of 25–54 focal planes are shown. The positions of the x-y images are indicated in the y-z images with yellow arrowheads, and those of the y-z images are indicated in the x-y images with magenta arrowheads. Scale bars, 10 μm.

Fig. 3. (continued)

overlaps (Supplemental Fig. S1B). Contrary to the nocodazole treatment of cells, air-drying did not affect mitotic progression (Fig. 2B). Co-immunostaining for α-tubulin, γ-tubulin, and centromeres (CREST) showed that microtubules around centrosomes and attached to kinetochores were detected in metaphase cells (Fig. 3). PRC1 stained at a tight midline in the center of the midzone and completely colocalized with α-tubulin in anaphase and telophase cells. In cells undergoing cytokinesis, α-tubulin staining was observed on the midbody and
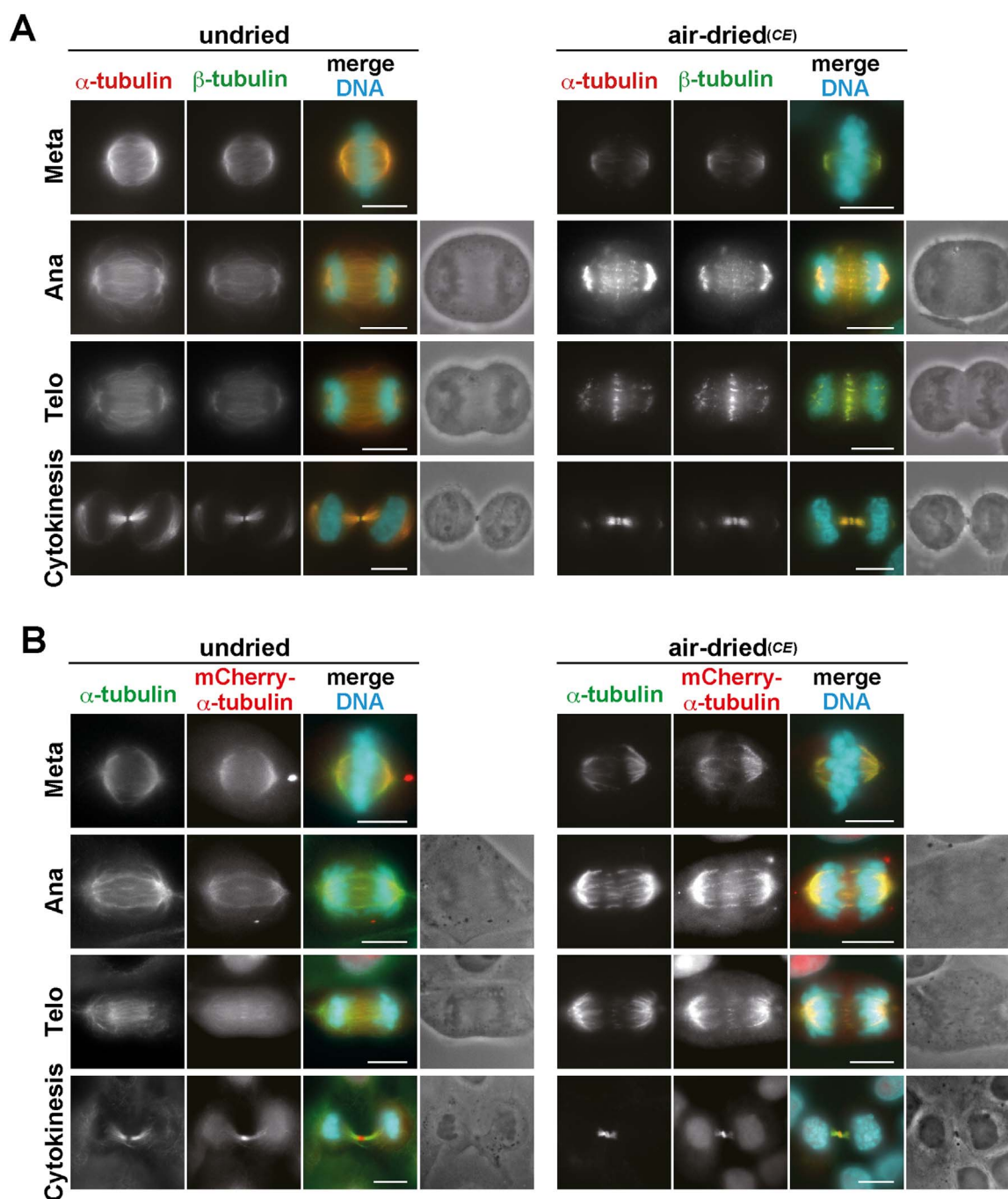
Fig. 4. Air-drying before fixation removes some populations of microtubules. (A) HeLa S3 cells were air-dried or undried, fixed with PTEMF, and stained for α-tubulin (red), β-tubulin (green), and DNA (cyan). Images show representative cells at the mitotic sub-phases. Phase-contrast images of cells are shown (right). (**B**) LLC-PK1 cells stably expressing mCherry-α-tubulin and EGFP-MKLP1 were air-dried or undried, fixed with PTEMF, and stained for α-tubulin (green) and DNA (cyan). An Alexa Fluor 647-conjugated secondary antibody was used to visualize α-tubulin. The microtubule fluorescence and mCherry in air-dried cells was contrast-enhanced (**CE**). The cells were classified into mitotic sub-phases as described in Fig. 1. Meta, metaphase; Ana, anaphase; Telo, telophase. Scale bars, 10 µm.

colocalized with Aurora B staining. These results suggest that air-drying the cells before fixation enables the visualization of antiparallel microtubule overlaps in the midzone and Flemming body.

Antiparallel microtubule overlaps were analyzed by confocal microscopy (Fig. 3B). The y-z views of the focal plane of undried cells showed different staining patterns for α-tubulin and PRC1, indicating that PRC1-positive antiparallel microtubule overlaps were not stained with the anti-α-tubulin antibody. In sharp contrast, PRC1 was almost completely colocalized with α-tubulin in the air-dried cells, confirming that air-drying before fixation enables visualization of antiparallel microtubule overlaps.

3.3. Microtubules, except antiparallel microtubule overlaps, are depolymerized by the air-drying method

Antiparallel microtubule overlaps in the spindle midzone and Flemming body, which are embedded in highly electron-dense matrices, were detected by the air-dry method, raising the possibility that the selective visualization of antiparallel microtubule overlaps is attributed to the enhancement of the antigenicity of α-tubulin in this region against the anti-α-tubulin antibody. Thus, we next stained air-dried cells with an anti-β-tubulin antibody. In the air-dried cells, β-
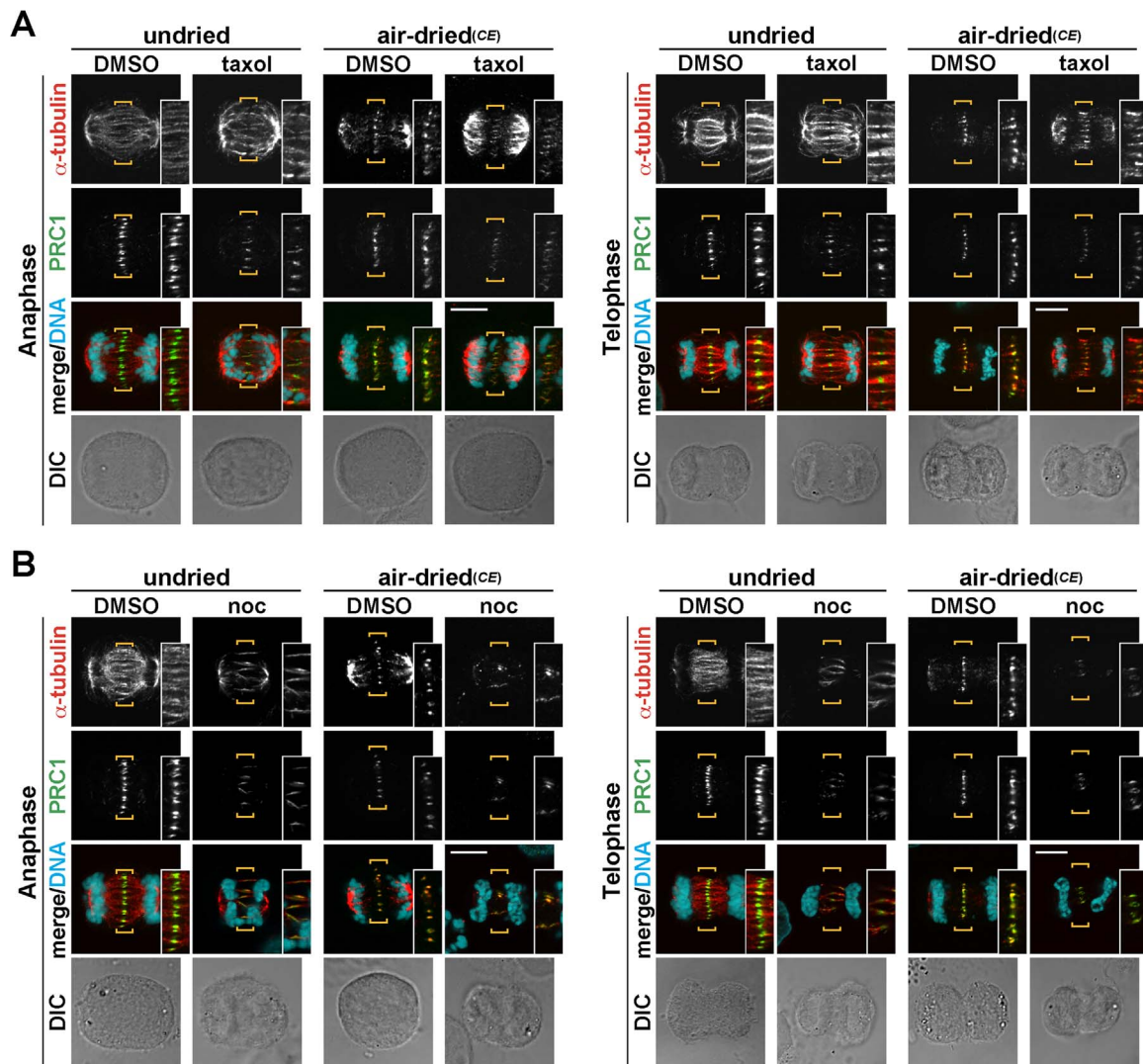
Fig. 5. Stable microtubules remain in the spindle midzone by air-drying of cells. HeLa S3 cells were treated with 8 µM RO-3306 for 20 h, washed free of RO-3306, and cultured in drug-free medium for 60 min. At the end of this incubation period, the cells were treated with DMSO (control) or 0.1 µg/mL Taxol for 5 min in (**A**), or DMSO (control) or 0.1 µg/mL nocodazole for 10 min in (**B**). Taxol-, nocodazole-, or solvent (DMSO)-treated cells were air-dried for 5 min or undried before fixation with PTEMF. The fixed cells were stained for α-tubulin (red), PRC1 (green), and DNA (cyan). The cells were classified into mitotic sub-phases as described in Fig. 1. Confocal images show representative cells at anaphase and telophase. The fluorescence of α-tubulin in air-dried cells was contrast-enhanced (**CE**). Magnified images are shown (right). DIC, differential interference contrast. Scale bars, 10 µm.

tubulin staining showed almost the same pattern as α-tubulin staining (Fig. 4A), suggesting that the alteration of the antigenicity of α-tubulin may not to be responsible for the characteristic staining of antiparallel microtubule overlaps.

We next used LLC-PK1 cells that stably express mCherry-α-tubulin at a lower level than endogenous α-tubulin (data not shown) and compared the fluorescence of mCherry-α-tubulin with the fluorescence of endogenous α-tubulin stained with the anti-α-tubulin antibody in air-dried cells. In undried cells, which were fixed with 4% formaldehyde, mCherry fluorescence, which was fused with α-tubulin, was almost the same as the fluorescence of the anti-α-tubulin antibody, except for the region of antiparallel microtubule overlaps and the Flemming body. mCherry-α-tubulin fluorescence, but not staining with the anti-α-tubulin antibody, was observed at the center of the midzone and Flemming body (Fig. 4B), supporting the view that the reactivity of the anti-tubulin antibody is blocked in the antiparallel microtubule overlaps in these regions by their being embedded in highly electron-dense matrices. In air-dried cells, mCherry-α-tubulin fluorescence was observed more clearly at the center of the anaphase and telophase midzone (Fig. 4B, right), suggesting that the selective visualization of antiparallel microtubule overlaps in the air-dried cells was not attributed

to the alteration of antigenicity, and raising the possibility that air-drying before fixation disrupts certain populations of microtubules, and, as a result, the antiparallel microtubule overlaps in the midzone and Flemming body are visualized as the remnant of microtubules. In metaphase LLC-PK1/mCherry-α-tubulin cells, almost all of the kinetochore microtubule lattice was detected in the air-dried cells (Fig. 4B, right), in contrast to HeLa S3 cells, in which only a portion of kinetochore microtubules were detected (Fig. 4A, right, see also Figs. 2A and 3). These results suggest that the effect of air-drying on mCherry-fused α-tubulin may differ somewhat from its effect on unfused α-tubulin.

To investigate the possibility that air-drying before fixation disrupts certain microtubule populations, excluding the antiparallel microtubule overlaps in the midzone and Flemming body, the cells were treated with the microtubule-stabilizing agent Taxol and then subjected to the air-drying method. As expected, Taxol treatment increased the fluorescence of α-tubulin staining in undried cells (Fig. 5A, Supplemental Fig. S2A). PRC1 staining was weakened, suggesting malfunctioning of the upstream regulators of PRC1. In the air-dried cells, longer microtubules were observed in the anaphase and telophase midzone, suggesting an increase in the resistance of microtubules to
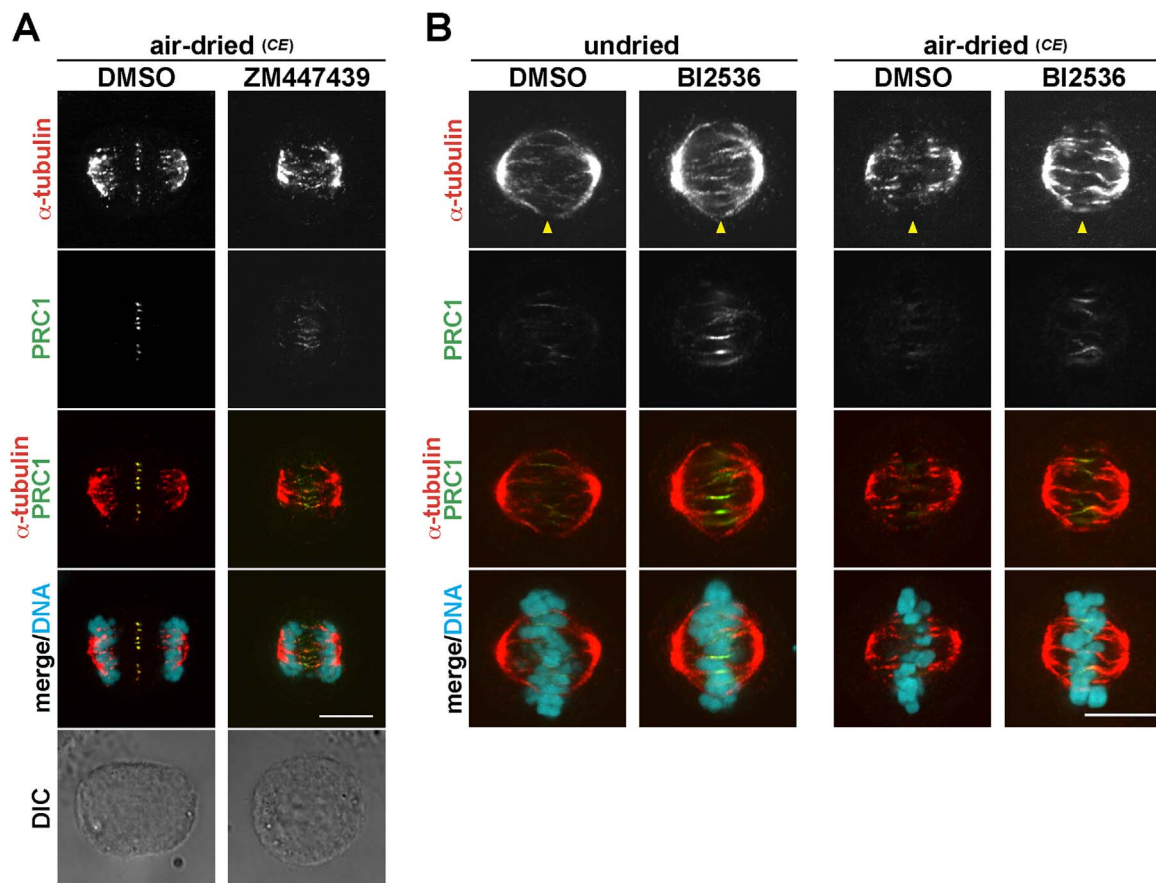
Fig. 6. Aurora B and Plk1 play roles in the regulation of the spindle midzone. HeLa S3 cells were treated with 8 μM RO-3306 for 20 h, washed free of RO-3306, and cultured in drug-free medium for 45 min. Then, the cells were treated with DMSO (control), 10 μM ZM447439 (**A**), or 0.1 μM BI2536 (**B**) for 15 min, and air-dried for 5 min or undried before fixation. After fixation with PTEMF, the cells were stained for α-tubulin (red), PRC1 (green), and DNA (cyan). Confocal images show representative cells at anaphase (**A**) or metaphase (**B**). The fluorescence of α-tubulin in air-dried cells was contrast-enhanced (**CE**). DIC, differential interference contrast. Scale bars, 10 μm.

depolymerization during air-drying. Furthermore, the cells were treated with the microtubule-depolymerizing agent nocodazole and stained for α-tubulin. As expected, nocodazole treatment decreased the fluorescence of α-tubulin staining in undried cells (Fig. 5B, Supplemental Fig. S2B). Similarly to treatment with Taxol, nocodazole treatment attenuated PRC1 staining in anaphase and telophase cells. In the air-dried cells, the number of microtubules was decreased in the anaphase and telophase midzone, indicating an increase in the sensitivity of microtubules to depolymerization during air-drying. Taken together, these results suggest that unstable microtubules are depolymerized during the air-drying method.

3.4. Detection of the effects of mitotic kinase inhibitors on midzone formation

By using the air-drying method, the effects of mitotic kinase inhibitors on antiparallel microtubule overlaps were examined. During anaphase, solvent control cells showed tightly aligned microtubules and PRC1 in the center of the central spindle (Fig. 6A, DMSO). In contrast, this was disrupted by Aurora B inhibition; PRC1-positive microtubules were detected, but not aligned (Fig. 6A, ZM447439). These results suggest that Aurora B inhibition abrogates midzone formation. By the conventional method, as shown in Fig. 1A, no clear difference was detected in the morphology of microtubules stained with the anti-α-tubulin antibody; however, an obvious difference was observed between Aurora B-inhibited and -uninhibited cells by the air-drying method (Fig. 6A). This suggests that the air-drying method is suitable for the detection of the effects of mitotic kinase inhibitors on the formation of antiparallel microtubule overlaps. We next treated the cells

with the Plk1 inhibitor BI2536 and found that PRC1 was localized at the microtubule bundles in the center region of undried metaphase cells upon Plk1 inhibition (Fig. 6B). This is in agreement with the observation that Plk1 prevents PRC1 from promoting premature midzone formation during metaphase by phosphorylating PRC1 at Thr602 [55]. Microtubule staining in the center region of undried cells was increased in addition to PRC1 by BI2536 treatment (Fig. 6B, undried). However, given that the disruption of signaling located upstream of PRC1 delocalizes PRC1 from antiparallel microtubule overlaps, as shown in Fig. 1A, it was unclear whether the increase in microtubule staining shown in Fig. 6B (undried) was caused by the formation of antiparallel microtubule overlaps. In air-dried cells, BI2536 treatment increased the number of microtubule filaments at the center region of cells (Fig. 6B, air-dried), indicating the formation of antiparallel microtubule overlaps. Therefore, this result revealed that the increase in microtubule staining by BI2536 treatment observed in undried cells (Fig. 6B, undried) could be attributed to the formation of antiparallel microtubule overlaps, which were bundled by PRC1. Taken together, these results suggest that the air-drying method is suitable for visualizing antiparallel microtubule overlaps in not only the anaphase and telophase midzone but also the premature midzone during metaphase.

4. Discussion

Whereas staining with an anti-tubulin antibody is used widely for morphological analyses of mitotic spindle microtubules, the detection of microtubules can be limited by the accessibility of the antibody to its epitope. For instance, the antiparallel microtubule overlaps in the midzone and Flemming body are microtubule populations that are

difficult to detect directly with an anti-tubulin antibody because of their dense structure. One solution to this problem is to express fluorescent protein-fused tubulin, enabling the visualization of these microtubule populations without using antibodies. However, it is sometimes problematic to obtain cell clones that stably express a fusion protein. Alternatively, staining of midzone-localizing proteins, including PRC1, is another way to visualize the midzone structure indirectly (Fig. 1A). PRC1 bundles the antiparallel microtubules and stabilizes the dense structure of the midzone [12]. However, PRC1 localization to the midzone requires its interaction with KIF4, which is phosphorylated by Aurora B [22,52]. Furthermore, Plk1 inhibition causes premature midzone formation during metaphase, and PRC1 localizes there [55]. These observations imply that aberrations in upstream regulators can cause PRC1 mislocalization (Fig. 1A) and that PRC1 is not suitable as a marker for antiparallel microtubule overlaps.

Microtubules in the antiparallel microtubule overlaps in the midzone and Flemming body are relatively stable; the enforced depolymerization of microtubules would have no effect on the stabilized microtubules of the midzone and midbody. To achieve this effect, we first tried to stain microtubules after cold treatment (Fig. 1B), which is known to depolymerize unstable microtubules [32]. However, midzone microtubules did not stain after cold treatment, suggesting that these microtubules are not tolerant to this treatment. As nocodazole treatment depolymerizes microtubules and the sensitivity to nocodazole varies among microtubule populations, we hypothesized that nocodazole treatment would selectively depolymerize unstable microtubules, and relatively stable populations of microtubules including the midzone and Flemming body would remain. However, nocodazole treatment affected mitotic progression; it decreased the number of anaphase and telophase cells (Fig. 1D). Besides, nocodazole treatment depolymerized the astral microtubules that generate the pulling force in anaphase B, causing morphological changes (Fig. 1C). Given that nocodazole treatment changed PRC1 localization in the midzone (Figs. 1C, 5B), it may affect the Aurora B-KIF4-PRC1 pathway, resulting in changes in morphology and mitotic progression. In the present study, we developed a novel and simple method to visualize microtubules with a highly dense structure, such as the antiparallel microtubule overlaps in the midzone and Flemming body; air-drying the cells before fixation enabled the detection of microtubules in these dense structures without affecting mitotic progression and morphology. Thus, we conclude that the air-drying method is suitable for staining the antiparallel microtubule overlaps in the midzone and Flemming body.

A lateral cross-sectional view constructed from z-stack images showed that the fluorescence of each focus increased upon cleavage furrow ingression (Supplemental Fig. S3A). However, quantification of fluorescence intensity revealed that the total intensity within an area of antiparallel microtubule overlaps was not statistically different between before and after cleavage furrow ingression (Supplemental Fig. S3B). Although further studies are required, these results suggest that microtubule bundles may be not resolved upon furrowing of the contractile ring and that the air-drying method will provide useful information on midzone microtubule arrangement upon furrowing.

Why does the air-drying method enable the visualization of microtubules in dense structures? We had considered two possibilities: enhancement of the antigenicity of tubulin or selective depolymerization of unstable microtubules. Analysis of mCherry-tubulin-expressing cells revealed that depolymerization of certain microtubule populations, but not enhancement of antigenicity, is responsible for the visualization of the midzone (Fig. 4). This is supported by the results obtained by using Taxol and nocodazole, in which Taxol treatment increased the number of microtubules detected by the air-drying method, while nocodazole treatment decreased this number (Fig. 5). Although nocodazole treatment causes morphological changes, the air-drying method, which also depolymerizes unstable microtubules, does not cause such changes. During air-drying, the cells may attach strongly to the cover slip at the chromosomes and midzone, preventing the midzone microtubules from

depolymerizing and undergoing morphological changes.

In conclusion, the air-drying of cells before fixation is a novel method suitable for staining microtubules in dense structures. Even if the regulators upstream of PRC1 malfunction and PRC1 mislocalizes, the air-drying method can provide images of microtubules in the antiparallel microtubule overlaps in the midzone and Flemming body. The midzone has crucial roles to guarantee accurate inheritance through the regulation of cytokinesis, and the method developed here can be applied to screen regulators and compounds that affect cytokinesis. Further analysis of the regulation of the midzone using the air-drying method will give insight into the mechanism underlying the proper progression of cytokinesis.

Author contributions

AI, TK, YS, and YN designed the study and wrote the paper. AI and YK performed all experiments. All authors reviewed the results and approved the final version of the manuscript.

Conflict of interest

The authors declare no conflict of interest.

Acknowledgments

Appendix A. Supplementary material

Supplementary data associated with this article can be found in the online version at http://dx.doi.org/10.1016/j.yexcr.2017.09.025.

References

[1] S. Etienne-Manneville, Microtubules in cell migration, Annu. Rev. Cell Dev. Biol. 29 (2013) 471–499, http://dx.doi.org/10.1146/annurev-cellbio-101011-155711.

[2] M.A. Welte, Bidirectional transport along microtubules, Curr. Biol. 14 (2004) 525–537, http://dx.doi.org/10.1016/j.cub.2004.06.045.

[3] S. Forth, T.M. Kapoor, The mechanics of microtubule networks in cell division, J. Cell Biol. 216 (2017) 1525–1531, http://dx.doi.org/10.1083/jcb.201612064.

[4] J. Fan, A.D. Griffiths, A. Lockhart, R.A. Cross, L.A. Amos, Microtubule minus ends can be labelled with a phage display antibody specific to alpha-tubulin, J. Mol. Biol. 259 (1996) 325–330, http://dx.doi.org/10.1006/jmbi.1996.0322.

[5] R.A. Walker, E.T. O'Brien, N.K. Pryer, M.F. Soboeiro, W.A. Voter, H.P. Erickson, et al., Dynamic instability of individual microtubules analyzed by video light microscopy: rate constants and transition frequencies, J. Cell Biol. 107 (1988) 1437–1448, http://dx.doi.org/10.1083/jcb.107.4.1437.

[6] A. Akhmanova, M.O. Steinmetz, Microtubule +TIPs at a glance, J. Cell Sci. 123 (2010) 3415–3419, http://dx.doi.org/10.1242/jcs.062414.

[7] G.S. Diamantopoulos, F. Perez, H.V. Goodson, G. Batelier, R. Melki, T.E. Kreis, et al., Dynamic localization of CLIP-170 to microtubule plus ends is coupled to microtubule assembly, J. Cell Biol. 144 (1999) 99–112, http://dx.doi.org/10.1083/jcb.144.1.99.

[8] Y. Komarova, C.O. De Groot, I. Grigoriev, S.M. Gouveia, E.L. Munteanu, J.M. Schober, et al., Mammalian end binding proteins control persistent microtubule growth, J. Cell Biol. 184 (2009) 691–706, http://dx.doi.org/10.1083/jcb.200807179.

[9] C.E. Walczak, S. Gayek, R. Ohi, Microtubule-depolymerizing kinesins, Annu. Rev. Cell Dev. Biol. 29 (2013) 417–441, http://dx.doi.org/10.1146/annurev-cellbio-101512-122345.

[10] K. Jiang, A. Akhmanova, Microtubule tip-interacting proteins: a view from both ends, Curr. Opin. Cell Biol. 23 (2011) 94–101, http://dx.doi.org/10.1016/j.ceb.

2010.08.008.

[11] J. Howard, A.A. Hyman, Microtubule polymerases and depolymerases, Curr. Opin. Cell Biol. 19 (2007) 31–35, http://dx.doi.org/10.1016/j.ceb.2006.12.009.

[12] C. Mollinari, J.P. Kleman, W. Jiang, G. Schoehn, T. Hunter, R.L. Margolis, PRC1 is a microtubule binding and bundling protein essential to maintain the mitotic spindle midzone, J. Cell Biol. 157 (2002) 1175–1186, http://dx.doi.org/10.1083/jcb. 200111052.

[13] V. Pavicic-Kaltenbrunner, M. Mishima, M. Glotzer, Cooperative assembly of CYK-4/ MgcRacGAP and ZEN-4/MKLP1 to form the centralspindlin complex, Mol. Biol. Cell 18 (2007) 4992–5003, http://dx.doi.org/10.1091/mbc.E07-05-0468.

[14] M. Mishima, S. Kaitna, M. Glotzer, Central spindle assembly and cytokinesis require a kinesin-like protein/RhoGAP complex with microtubule bundling activity, Dev. Cell 2 (2002) 41–54 ⟨http://www.ncbi.nlm.nih.gov/pubmed/11782313⟩.

[15] J. Matuliene, R. Kuriyama, Kinesin-like protein CHO1 is required for the formation of midbody matrix and the completion of cytokinesis in mammalian cells, Mol. Biol. Cell 13 (2002) 1832–1845 (doi:01-10-0504).

[16] S.V. Bratman, F. Chang, Stabilization of overlapping microtubules by fission yeast CLASP, Dev. Cell. 13 (2007) 812–827, http://dx.doi.org/10.1016/j.devcel.2007.10. 015.

[17] H. Maiato, E.A.L. Fairley, C.L. Rieder, J.R. Swedlow, C.E. Sunkel, W.C. Earnshaw, Human CLASP1 is an outer kinetochore component that regulates spindle micro-tubule dynamics, Cell 113 (2003) 891–904, http://dx.doi.org/10.1016/S0092-8674(03)00465-3.

[18] A. Akhmanova, C.C. Hoogenraad, K. Drabek, T. Stepanova, B. Dortland, T. Verkerk, et al., CLASPs are CLIP-115 and -170 associating proteins involved in the regional regulation of microtubule dynamics in motile fibroblasts, Cell 104 (2001) 923–935, http://dx.doi.org/10.1016/S0092-8674(01)00288-4.

[19] U. Gruneberg, R. Neef, R. Honda, E.A. Nigg, F.A. Barr, Relocation of Aurora B from centromeres to the central spindle at the metaphase to anaphase transition requires MKlp2, J. Cell Biol. 166 (2004) 167–172, http://dx.doi.org/10.1083/jcb. 200403084.

[20] R. Neef, C. Preisinger, J. Sutcliffe, R. Kopajtich, E.A. Nigg, T.U. Mayer, et al., Phosphorylation of mitotic kinesin-like protein 2 by polo-like kinase 1 is required for cytokinesis, J. Cell Biol. 162 (2003) 863–875, http://dx.doi.org/10.1083/jcb. 200306009.

[21] P. Bieling, I.A. Telley, T. Surrey, A minimal midzone protein module controls for-mation and length of antiparallel microtubule overlaps, Cell 142 (2010) 420–432, http://dx.doi.org/10.1016/j.cell.2010.06.033.

[22] C.K. Hu, M. Coughlin, C.M. Field, T.J. Mitchison, KIF4 regulates midzone length during cytokinesis, Curr. Biol. 21 (2011) 815–824, http://dx.doi.org/10.1016/j. cub.2011.04.019.

[23] Y. Kurasawa, W.C. Earnshaw, Y. Mochizuki, N. Dohmae, K. Todokoro, Essential roles of KIF4 and its binding partner PRC1 in organized central spindle midzone formation, EMBO J. 23 (2004) 3237–3248, http://dx.doi.org/10.1038/sj.emboj. 7600347.

[24] C. Zhu, W. Jiang, Cell cycle-dependent translocation of PRC1 on the spindle by Kif4 is essential for midzone formation and cytokinesis, Proc. Natl. Acad. Sci. USA 102 (2005) 343–348, http://dx.doi.org/10.1073/pnas.0408438102.

[25] M.E. Douglas, M. Mishima, Still entangled: assembly of the central spindle by multiple microtubule modulators, Semin. Cell Dev. Biol. 21 (2010) 899–908, http://dx.doi.org/10.1016/j.semcdb.2010.08.005.

[26] R.A. Green, E. Paluch, K. Oegema, Cytokinesis in animal cells, Annu. Rev. Cell Dev. Biol. 28 (2012) 29–58, http://dx.doi.org/10.1146/annurev-cellbio-101011-155718.

[27] E.N. Cytrynbaum, J.M. Scholey, A. Mogilner, A force balance model of early spindle pole separation in Drosophila embryos, Biophys. J. 84 (2003) 757–769, http://dx. doi.org/10.1016/S0006-3495(03)74895-4.

[28] M.E. Tanenbaum, R.H. Medema, Mechanisms of centrosome separation and bipolar spindle assembly, Dev. Cell. 19 (2010) 797–806, http://dx.doi.org/10.1016/j. devcel.2010.11.011.

[29] H.J. Nam, R.M. Naylor, J.M. van Deursen, Centrosome dynamics as a source of chromosomal instability, Trends Cell Biol. 25 (2015) 65–73, http://dx.doi.org/10. 1016/j.tcb.2014.10.002.

[30] J.G. DeLuca, W.E. Gall, C. Ciferri, D. Cimini, A. Musacchio, E.D. Salmon, Kinetochore microtubule dynamics and attachment stability are regulated by Hec1, Cell 127 (2006) 969–982, http://dx.doi.org/10.1016/j.cell.2006.09.047.

[31] S.C. Sweet, M.J. Welsh, Calmodulin colocalization with cold-stable and nocodazole-stable microtubules in living PtK1 cells, Eur. J. Cell Biol. 47 (1988) 88–93 ⟨http://www.ncbi.nlm.nih.gov/pubmed/3068060⟩ (Accessed 27 May 2017).

[32] B.R. Brinkley, J. Cartwright, Cold-labile and cold-stable microtubules in the mitotic spindle of mammalian cells, Ann. N.Y. Acad. Sci. 253 (1975) 428–439, http://dx. doi.org/10.1111/j.1749-6632.1975.tb19218.x.

[33] C.L. Rieder, The structure of the cold-stable kinetochore fiber in metaphase PtK1 cells, Chromosoma 84 (1981) 145–158 ⟨http://www.ncbi.nlm.nih.gov/pubmed/

7297248⟩ (Accessed 27 May 2017).

[34] J.G. DeLuca, B. Moree, J.M. Hickey, J.V. Kilmartin, E.D. Salmon, hNuf2 inhibition blocks stable kinetochore-microtubule attachment and induces mitotic cell death in HeLa cells, J. Cell Biol. 159 (2002) 549–555, http://dx.doi.org/10.1083/jcb. 200208159.

[35] I. Brust-Mascher, G. Civelekoglu-Scholey, M. Kwon, A. Mogilner, J.M. Scholey, Model for anaphase B: role of three mitotic motors in a switch from poleward flux to spindle elongation, Proc. Natl. Acad. Sci. USA 101 (2004) 15938–15943, http://dx. doi.org/10.1073/pnas.0407044101.

[36] J. Scholey, G. Civelekoglu-Scholey, I. Brust-Mascher, B. Anaphase, Biology 5 (2016) 51, http://dx.doi.org/10.3390/biology5040051.

[37] I. Brust-Mascher, J.M. Scholey, Mitotic motors and chromosome segregation: the mechanism of anaphase B: figure 1, Biochem. Soc. Trans. 39 (2011) 1149–1153, http://dx.doi.org/10.1042/BST0391149.

[38] N.J. Ganem, Z. Storchova, D. Pellman, Tetraploidy, aneuploidy and cancer, Curr. Opin. Genet Dev. 17 (2007) 157–162.

[39] N.J. Ganem, S.A. Godinho, D. Pellman, A mechanism linking extra centrosomes to chromosomal instability, Nature 460 (2009) 278–282, http://dx.doi.org/10.1038/ nature08136.

[40] M. Fujiwara, M. Bandi, M. Nitta, E.V. Ivanova, R.T. Bronson, D. Pellman, Cytokinesis failure generating tetraploids promotes tumorigenesis in p53-null cells, Nature 437 (2005) 1043–1047, http://dx.doi.org/10.1038/nature04217.

[41] Z. Storchová, A. Breneman, J. Cande, J. Dunn, K. Burbank, E. O'Toole, et al., Genome-wide genetic analysis of polyploidy in yeast, Nature 443 (2006) 541–547, http://dx.doi.org/10.1038/nature05178.

[42] Y. Nakayama, S. Soeda, M. Ikeuchi, K. Kakae, N. Yamaguchi, Cytokinesis failure leading to chromosome instability in v-Src-induced oncogenesis, Int. J. Mol. Sci. 18 (2017) 811, http://dx.doi.org/10.3390/ijms18040811.

[43] J.M. Mullins, J.J. Biesele, Terminal phase of cytokinesis in D-98s cells, J. Cell Biol. 73 (1977) 672–684 ⟨http://jcb.rupress.org/content/jcb/73/3/672.full.pdf⟩ (Accessed 28 April 2017).

[44] W.M. Saxton, J.R. McIntosh, Interzone microtubule behavior in late anaphase and telophase spindles, J. Cell Biol. 105 (1987) 875–886 ⟨http://jcb.rupress.org/ content/jcb/105/2/875.full.pdf⟩ (Accessed 28 April 2017).

[45] M. Abe, A. Makino, F. Hullin-Matsuda, K. Kamijo, Y. Ohno-Iwashita, K. Hanada, et al., A role for sphingomyelin-rich lipid domains in the accumulation of phos-phatidylinositol-4,5-bisphosphate to the cleavage furrow during cytokinesis, Mol. Cell. Biol. 32 (2012) 1396–1407, http://dx.doi.org/10.1128/MCB.06113-11.

[46] E. Iwamoto, N. Ueta, Y. Matsui, K. Kamijo, T. Kuga, Y. Saito, et al., ERK plays a role in chromosome alignment and participates in M-phase progression, J. Cell. Biochem. 117 (2016) 1340–1351, http://dx.doi.org/10.1002/jcb.25424.

[47] K. Kakae, M. Ikeuchi, T. Kuga, Y. Saito, N. Yamaguchi, Y. Nakayama, v-Src-induced nuclear localization of YAP is involved in multipolar spindle formation in tetraploid cells, Cell Signal. 30 (2017) 19–29, http://dx.doi.org/10.1016/j.cellsig.2016.11. 014.

[48] Y. Nakayama, A. Igarashi, I. Kikuchi, Y. Obata, Y. Fukumoto, N. Yamaguchi, Bleomycin-induced over-replication involves sustained inhibition of mitotic entry through the ATM/ATR pathway, Exp. Cell Res. 315 (2009) 2515–2528, http://dx. doi.org/10.1016/j.yexcr.2009.06.007.

[49] Y. Nakayama, Y. Matsui, Y. Takeda, M. Okamoto, K. Abe, Y. Fukumoto, et al., c-Src but not Fyn promotes proper spindle orientation in early prometaphase, J. Biol. Chem. 287 (2012) 24905–24915, http://dx.doi.org/10.1074/jbc.M112.341578.

[50] Y. Nakayama, Y. Saito, S. Soeda, E. Iwamoto, S. Ogawa, N. Yamagishi, et al., Genistein induces cytokinesis failure through RhoA delocalization and anaphase chromosome bridging, J. Cell. Biochem. 115 (2014) 763–771, http://dx.doi.org/10. 1002/jcb.24720.

[51] E. Iwamoto, N. Ueta, Y. Matsui, K. Kamijo, T. Kuga, Y. Saito, et al., ERK plays a role in chromosome alignment and participates in M-phase progression, J. Cell. Biochem. 117 (2016) 1340–1351, http://dx.doi.org/10.1002/jcb.25424.

[52] R.N. Bastos, S.R. Gandhi, R.D. Baron, U. Gruneberg, E.A. Nigg, F.A. Barr, Aurora B suppresses microtubule dynamics and limits central spindle size by locally acti-vating KIF4A, J. Cell Biol. 202 (2013) 605–621, http://dx.doi.org/10.1083/jcb. 201301094.

[53] L. Liu, S. Tommasi, D.-H. Lee, R. Dammann, G.P. Pfeifer, Control of microtubule stability by the RASSF1A tumor suppressor, Oncogene 22 (2003) 8125–8136, http://dx.doi.org/10.1038/sj.onc.1206984.

[54] G. Wu, Y.-T. Lin, R. Wei, Y. Chen, Z. Shan, W.-H. Lee, Hice1, a novel microtubule-associated protein required for maintenance of spindle integrity and chromosomal stability in human cells, Mol. Cell. Biol. 28 (2008) 3652–3662, http://dx.doi.org/ 10.1128/MCB.01923-07.

[55] C.-K.K. Hu, N. Ozlu, M. Coughlin, J.J. Steen, T.J. Mitchison, Plk1 negatively reg-ulates PRC1 to prevent premature midzone formation before cytokinesis, Mol. Biol. Cell. 23 (2012) 2702–2711, http://dx.doi.org/10.1091/mbc.E12-01-0058.